Copy No.

10

NASA GENERAL WORKING PAPER NO. 10 043

EXPERIMENTAL ABLATION DATA OBTAINED FROM MSC ONE MEGAWATT ARC JET TESTS ON THE STANFORD RESEARCH INSTITUTE - NASA ROUND ROBIN ABLATION PROGRAM

NATIONAL AERONAUTICS AND SPACE ADMINISTRATION

MANNED SPACECRAFT CENTER

HOUSTON, TEXAS

March 30, 1965

18 1965

NASA GENERAL WORKING PAPER NO. 10 043

EXPERIMENTAL ABLATION DATA OBTAINED FROM MSC ONE MEGAWATT

ARC JET TESTS ON THE STANFORD RESEARCH INSTITUTE -

NASA ROUND ROBIN ABLATION PROGRAM

Pre_ ~ed by: Donald J. Tillian
D. J. Tillian
AST, Entry Environment Simulation Section

Authorized for Distribution:

Warren Gillespie, Jr.
for Maxime A. Faget
Assistant Director for Engineering and Development

NATIONAL AERONAUTICS AND SPACE ADMINISTRATION

MANNED SPACECRAFT CENTER

HOUSTON, TEXAS

March 30, 1965

TABLE OF CONTENTS

LIST OF TABLES

LIST OF FIGURES

EXPERIMENTAL ABLATION DATA OBTAINED FROM MSC ONE MEGAWATT ARC JET TESTS ON THE STANFORD RESEARCH INSTITUTE - NASA ROUND ROBIN ABLATION PROGRAM

By D. J. Tillian

INTRODUCTION

The purpose of this paper is to present experimental ablation data from arc jet tests conducted at the Manned Spacecraft Center (MSC) as part of the NASA round robin ablation program. This program was conducted to determine and correlate the differences in test results obtained in the current arc heated materials testing facilities in the country. The program is being managed for the National Aeronautics and Space Administration (NASA) by the Stanford Research Institute (SRI) under Contract No. NASr-49(15). Along with MSC, other participating organizations in this program include the Ames Research Center (ARC), the Langley Research Center (LRC), the Wright Patterson Air Force Base (WPAFB), the Giannini Scientific Corporation, the Avco Corporation, the Boeing Company, the North American Aviation Inc. (NAA), the General Electric Company (GE), the Martin Marietta Corporation, and the Cincinnati Testing Laboratories (CTL).

A standard heat transfer rate calorimeter, total pressure probe, and a set of 10 ablation models were furnished each facility for ablation tests. The test matrix selected for each of the participating organizations, with the exception of CTL, is shown in table I (see ref. 1).

The overlapping test conditions in the various facilities is expected to provide a meaningful correlation between ablation material results in the different arc heated facilities.

All of the organizations, with the exception of MSC, conducted the ablation material tests in a vacuum and under supersonic flow conditions. The MSC facility differs in that the tests are conducted at atmospheric pressure using a subsonic velocity stream.

This paper contains only the data from the Manned Spacecraft Center facility. The ablation data from the other participating organizations along with the MSC data will be reported by the Stanford Research Institute.

SYMBOLS

c_p specific heat at constant pressure – Btu/lb°F

E arc voltage – volts

H_A heat of ablation – Btu/lb

H_D heat of degradation – Btu/lb

H_T total enthalpy of gas stream – Btu/lb

I arc current – amperes

k thermal conductivity – Btu/ft^2 °F/ft

l thickness – ft

M mass flow – lb/sec

$\dot{m}$ ablation rate – lb/ft^2-sec

q heat transfer rate – Btu/ft^2-sec

R radius – ft

T temperature – °F

t time – sec

ρ density – lb/ft^3

Subscripts:

w water

g gas

h hot wall

c cold wall

MATERIAL SPECIMENS

Two different types of materials were selected for testing in arc heated materials testing facilities. The materials were: (1) teflon, type TFE, white variety, density of 135 lb/ft^3, and (2) phenolic nylon, 50 percent phenolic, 50 percent nylon by weight, density of 75 lb/ft^3. These materials were chosen because they represented the low and high temperature classes of ablators.

The materials required for the construction of the models were furnished by NASA. The materials were machined as flat face cylindrical models as shown in figure 1. Each model contained one chromel-alumel thermocouple for recording back surface temperature.

TEST FACILITY

The facility used by MSC in this program was the one megawatt arc jet as shown in figure 2. The arc jet utilizes water cooled electrodes, constrictor, and nozzles. Nitrogen is injected at the base of the cathode and oxygen is injected in the anode region. The heated gas stream exits through a 3-inch diameter water cooled subsonic nozzle. The facility is equipped with two hydraulic specimen inserters for positioning of the models and heat transfer rate sensors in the arc jet stream.

Heat transfer rates were measured during each run by an asymptotic calorimeter manufactured by the Hy-Cal Corporation. Other equipment used during this program include a Milliken camera operating at 16 frames per second for recording specimen appearance during a test, an optical pyrometer and a radiometer for specimen surface temperature measurements, and an oscillograph for recording model back face temperatures. All of the pertinent operating conditions of the arc jet and the calorimeter and model data were recorded on magnetic tape in digital form.

ARC JET STREAM CALIBRATION

Prior to the model tests, an extensive calibration program was conducted using the SRI calorimeter, a Hy-Cal calorimeter, and a MSC-designed copper slug calorimeter. The sensing element in the MSC and SRI calorimeter was constructed of copper with a chromel alumel thermocouple attached to the back surface. All the calorimeters used in these tests had the same effective nose radius.

Analysis of heat transfer rates from the copper slug calorimeter data is based on the specific heat of the copper disc and the rate of temperature rise of the disc. The heat transfer rates were determined by the following equation:

$$q = (C_p \rho l) \frac{dT}{dt}$$

The Hy-Cal Corporation asymptotic calorimeter is the standard heat transfer rate sensor utilized in the MSC facility. This sensor differs from the conventional slug type calorimeter in that it measures a temperature gradient between the center and periphery of a thin constantan disc. This temperature differiential is directly proportional to the heating rate and is expressed in the following equation:

$$q = \frac{4lk}{R^2} \Delta T$$

Comparison data of the heating rates measured by the MSC slug calorimeter, SRI calorimeter, and the Hy-Cal calorimeter is shown in table II. A comparison is shown in figure 3 where the heating rate measured by the Hy-Cal calorimeter is plotted against that measured using slug type calorimeters. It can be seen that good agreement within ±5 percent was obtained between the different types of calorimeters.

The enthalpy of the gas stream was determined by the energy balance technique. The average total enthalpy can be readily established using the following experimental data:

1. Electrical power to the arc generator
2. Total gas flow into the arc generator
3. Cooling water flow rates
4. Cooling water inlet and exit temperatures.

The equation takes the form:

$$H_{avg} = \frac{(.948\ IE) - (M_w C_{\rho w}\ \Delta Tw)}{Mg}$$

MATERIALS EVALUATION

Teflon

For the evaluation of the teflon data, the conventional parameter termed the effective heat of ablation was calculated for each model. The equation takes the form:

$$H_a = \frac{q_h}{m}$$

The heat of ablation data for the teflon models is presented as a function of enthalpy potential in figure 4. Prior to the initiation of the SRI tests, a number of teflon models similar in design to the SRI models were fabricated and tested. The experimental data obtained during these tests are shown in table III. The results of these tests are also shown in figure 4. An analytical prediction of the heat of ablation based on the theory of reference 2 and experimental data from the Langley Research Center (ref. 3) is shown in figure 4 for comparison with the test results obtained from the MSC arc-heated facility.

Phenolic Nylon

The heat of ablation and heat of degradation based on cold wall heating rate was calculated for each phenolic nylon model and is presented in figure 5. The heat of degradation was calculated in the same manner as the heat of ablation except the mass loss rate ($\dot{m}$) included the char weight and recession weight loss. Surface temperatures of the models are shown in figure 6 as a function of cold wall heating rate.

RESULTS

The experimental data obtained on the material tests during the SRI program are summarized in tables IV and V. Photographs of the tested models are shown in figures 7 through 10.

Over the range of the test conditions obtained during this program, the three different heating rate sensors agreed within ±5 percent. The first calorimeter received from SRI exhibited a greater deviation (approximately 25 percent). It is believed that this calorimeter was damaged prior to the higher heating rate tests. A second calorimeter was obtained from SRI and good agreement was obtained between this calorimeter and the Hy-Cal calorimeter.

The heat of ablation data for teflon shows reasonable agreement with theory. Due to the small number of teflon tests which were conducted during this program, a quantitative interpretation of the results was not made. However, the teflon data demonstrates the feasibility of the utilization of experimental ablation data for the determination of enthalpy of an arc heated gas stream.

Comparison of the phenolic nylon experimental data with theoretical analysis was not undertaken in this paper because of the problem of defining char removal mechanisms. Comparative experimental data were not available in the literature due to the unique testing capabilities of the MSC arc jet facility. The MSC experimental data demonstrates the significant effect of heating rate on the thermal performance of a charring ablator which is in agreement with tests conducted in other test facilities at lower pressure levels. Measurements of the mass loss rate of phenolic nylon by the various organizations participating in the SRI program should provide an insight into external pressure effects on this class of ablator.

CONCLUDING REMARKS

Interpretation of the ablation data obtained during this program is being conducted by the Stanford Research Institute. The results from this material test program should provide a sound basis for evaluation of ablation results from various arc jet facilities. It should also permit a greater degree of confidence in predicting flight performance from the ground test results.

REFERENCES

1. Hiester, Nevin K., and Clark, Carroll F.: Feasibility of Simulating Thermal Environments for Meaningful Evaluation of Ablating Materials, Quarterly Progress Report No. IV, February 1- April 30, 1964, Contract No. NAS R-49(15).

2. Georgiev, Steven; Hidalgo, Henry; and Adams, Mac C.: On Ablating Heat Shields for Satellite Recover, Avco- Everett Research Report 65, July 1959.

3. Chapman, Andrew J.: An Experimental Investigation of Several Ablation Materials in an Electric-Arc-heated Air Jet, NASA TN D-1520, April 1963.

4. Adams, Mac C.: Recent Advances in Ablation ARS Journal Vol 29, No. 9, September 1959.

TABLE I.- TEST CONDITIONS FOR PARTICIPATING ORGANIZATIONS

Enthalpy, Btu/lb	Heat rate, Btu/ft^{2}sec	ARC	LRC	MSC	WPAFB FMD	Giannini	Avco	Martin	Boeing	NAA	GE
1 500	30	T	T P		T					T	
1 500	40										
1 700	60		T								
3 000	40							T			
3 000	60	T	T P		T	T				T P	
3 000	90		P							T P	
3 000	125									P	T
4 500	90		T P								
5 000	50					T P	T P	T P			T P
5 000	100	T P			T P	T P	T P	T P			
5 000	130					P		P		T P	T P
5 000	150	P			P						
5 000	200	T P			T P						
5 000	300			T P	P				T P		
5 000	470			P					P		
5 000	600								P		
6 500	170									T P	
7 000	140				T P						
7 500	150	T P		T P							
7 500	500	P									
8 500	180									T P	
10 000	100					P	T P	T P			
10 000	200					T	T				
10 000	300								T		
10 000	500			T P							
10 000	900			T							
12 000	250							T P			
13 000	80										P
13 000	270										T P
13 500	900			T P							
15 000	150						P				
15 000	300					T P	T P		T P		
15 000	470										

T is a teflon model

P is a phenolic nylon model

TABLE II. - CALORIMETER CALIBRATION DATA

Run number	Enthalpy Btu/lb	Total pressure, Atm	Heat flux $\dot{q}$ Hy-Cal, Btu/ft^{2}sec	Heat flux $\dot{q}$ SRI-Cal, Btu/ft^{2}sec	Heat flux $\dot{q}$ MSC-slug, Btu/ft^{2}sec	Power to arc, Btu/sec	Calorimeter distance from nozzle, in.
151	11 515	1.0	669		668	714.3	2.0
154	5 303	1.0	265		276	310.7	2.0
	5 645	1.0	275		258		
155	4 830	1.0	315		331	296.4	1.5
	6 568	1.0	470		463	404.8	1.5
	11 638	1.0	652		616	728.6	1.5
160	5 223	1.0	330	331		308.6	1.5
	7 505	1.0	497	381		414.3	1.5
	13 300	1.0	778	698		744.3	1.5
	5 486	1.0	337	275		316.4	1.5
161	5 760	1.0		283	280	308.6	1.5
	5 380	1.0		296	323	308.6	1.5
164	5 440	1.0		181	307	317.9	1.5
	7 200	1.0			443	434.3	1.5
	13 833	1.0			794	731.4	1.5
[a]188	5 025	1.0	137	134		299.3	1.5
	6 525	1.0	345	325		395.2	1.5
	11 681	1.0	550	504		681.4	1.5
	5 025	1.0	137	125		296.4	1.5
189	4 800	1.0				299.3	1.5
	6 075	1.0	350			395.2	1.5
	10 612	1.0	568			681.4	1.5
	4 650	1.0	185			296.4	1.5

[a]SRI calorimeter no. 5

TABLE III.- TEFLON CALIBRATION DATA

Run number	Model number	Model test time, sec	Heat flux $\dot{q}$ Hy-Cal, Btu/ft^{2}sec	Enthalpy, Btu/lb	Total pressure, Atm	Power to arc, Btu/sec	Model distance from nozzle, in.	Model weight loss, lbs	Model surface area, ft^2
144	1	18.1	783	13 273	1.0	764.3	2.0	.005019	.00214
145	2	34.2	300	4 266	1.0	234.3	2.0	.007225	.00214
156	3	28.8	280	5 001	1.0	290.0	1.5	.005062	.00214
157	4	29.8	529	8 378	1.0	502.9	1.5	.007473	.00214
158	5	29.2	657	13 146	1.0	742.9	1.5	.007919	.00214
165	6	31.9	320	5 864	1.0	316.4	1.5	.005759	.00214
166	7	31.0	506	7 419	1.0	430.5	1.5	.007473	.00214
167	8	27.8	793	13 043	1.0	758.6	1.5	.008703	.00214

TABLE IV. - MODEL TEST DATA

Run number	Model number	Model test time, sec	Heat flux $\dot{q}$ Hy-Cal Btu/ft^{2}sec	Enthalpy Btu/lb	Model* surface temp ($^\circ$F)	Total pressure, Atm	Power to arc, Btu/sec	Model distance from nozzle, in.	Gas flow, lb/sec
168	P4B6	22.0	316	5 064	4025	1.0	307.9	1.5	.04
169	P9A4	8.5	350	5 281	-	1.0	315.0	1.5	.04
170	P4B7	4.6	413	5 424	-	1.0	321.4	1.5	.04
171	T-53	31.7	436	5 493	1500	1.0	322.9	1.5	.04
172	T-48	29.4	525	8 818	400	1.0	459.2	1.5	.04
173	P4B5	30.3	534	7 527	4342	1.0	454.3	1.5	.04
174	T-54	29.4	528	7 500	1900	1.0	452.4	1.5	.04
175	P4B2	12.8	540	7 701	4430	1.0	461.9	1.5	.04
176	P4B4	30.2	478	6 037	5070	1.0	350.0	1.5	.04
177	T-51	30.0	807	12 449	-	1.0	771.4	1.5	.04
178	P9A3	20.0	746	12 068	5025	1.0	755.7	1.5	.04
180	T-47	31.3	300	5 000	900	1.0	300.7	1.5	.04
184	P8B2	32.7	295	5 800	4218	1.0	378.0	1.5	.04
185	P8B5	15.0	295	5 800	3820	1.0	380.9	1.5	.04
186	P8B6	10.0	300	5 876	3733	1.0	385.0	1.5	.04
187	P8B4	31.9	115	4 570	3552	1.0	289.3	1.5	.04

*NOTE: ϵ = .8 phenolic nylon models – optical pyrometer
ϵ = 1.0 teflon model – radiometer

TABLE V. - MODEL MEASUREMENTS DATA

Model number	Model core weight loss, gm	Char weight, gm	Mass loss per area, lb/ft^2	Model core length initial, in.	Model core length final, in.	Recession, in.	Char thickness, in.	Pyrolysis zone, in.
T 47	1.995		2.07	0.750	0.566	0.184		
T 48	3.290		3.41	.750	.445	.305		
T 51	4.221		4.36	.751	.362	.389		
T 53	3.200		3.31	.751	.455	.296		
T 54	3.329		3.45	.751	.448	.303		
P4B2	.623	.275	.645	.751	.723	.028	.104	.050
P4B4	1.184	.456	1.228	.751	.666	.085	.160	.083
P4B5	1.271	.483	1.319	.754	.662	.092	.192	.075
P4B6	.728	.324	.745	.755	.725	.030	.127	.070
P4B7	.213	.079	.221	.756	.752	.004	.037	.020
P8B2	.973	.456	1.008	.755	.698	.057	.156	.075
P8B4	.570	.248	.590	.757	.761	+.004	.108	.080
P8B5	.504	.243	.522	.757	.738	.019	.090	.045
P8B6	1.227	.270	1.270	.756	.695	.061	.163	.082
P9A3	1.059	.407	1.095	.749	.676	.073	.145	.055
P9A4	.345	.129	.357	.751	.746	.005	.062	.030

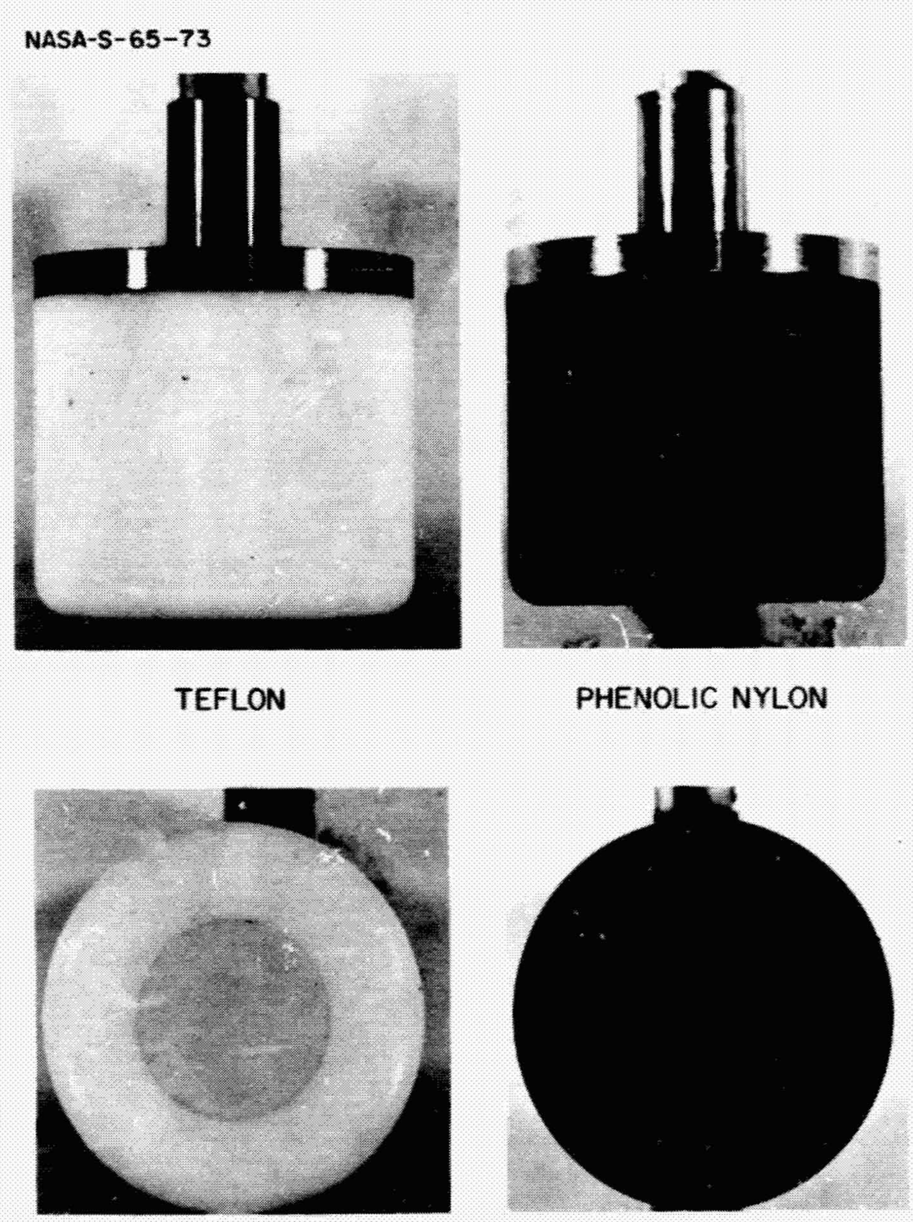

Figure 1.- Front and side views of phenolic nylon and teflon models before test.

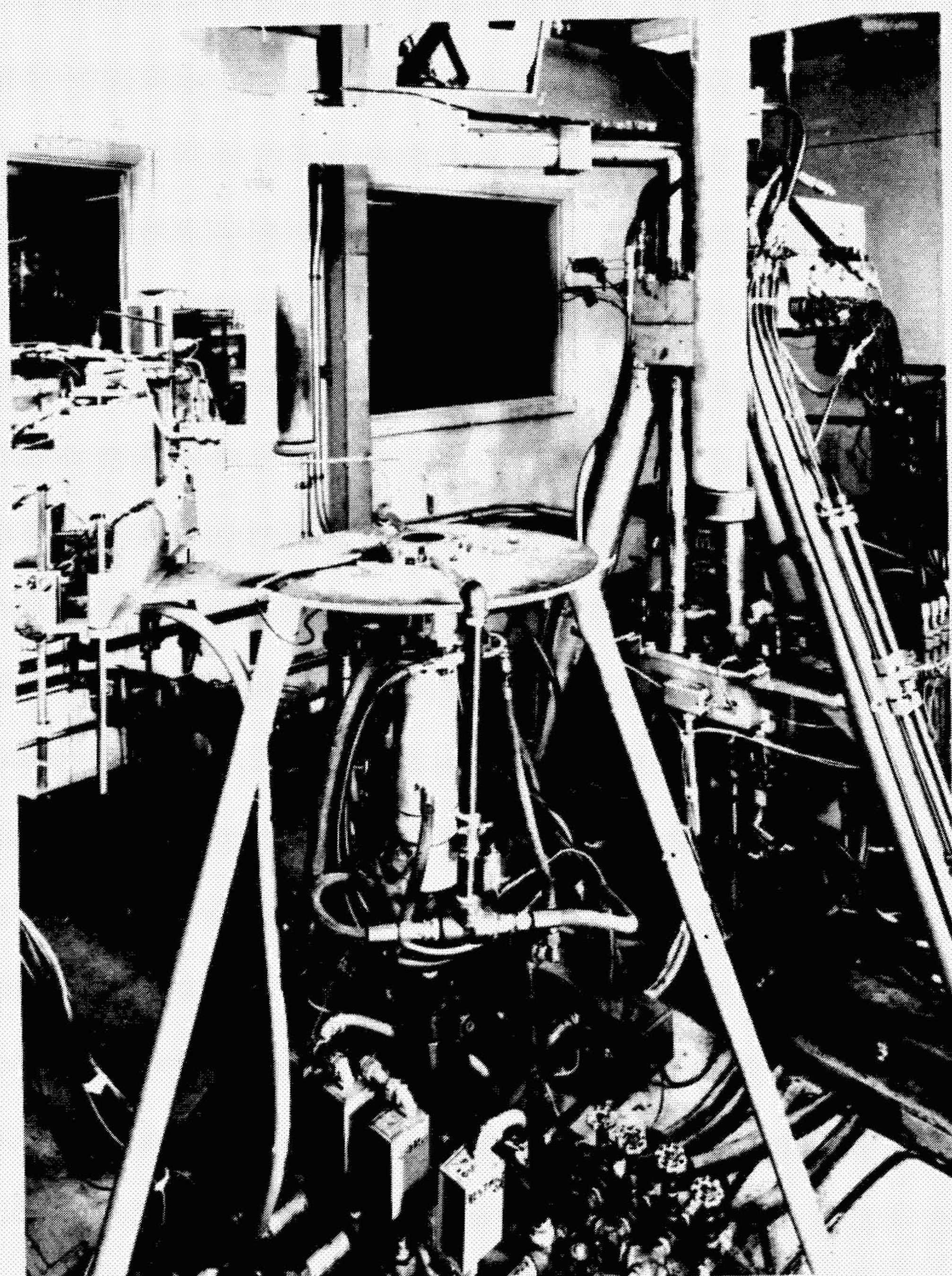

NASA
S-65-17522

Figure 2.- One megawatt arc-jet facility.

NASA-S-65-65

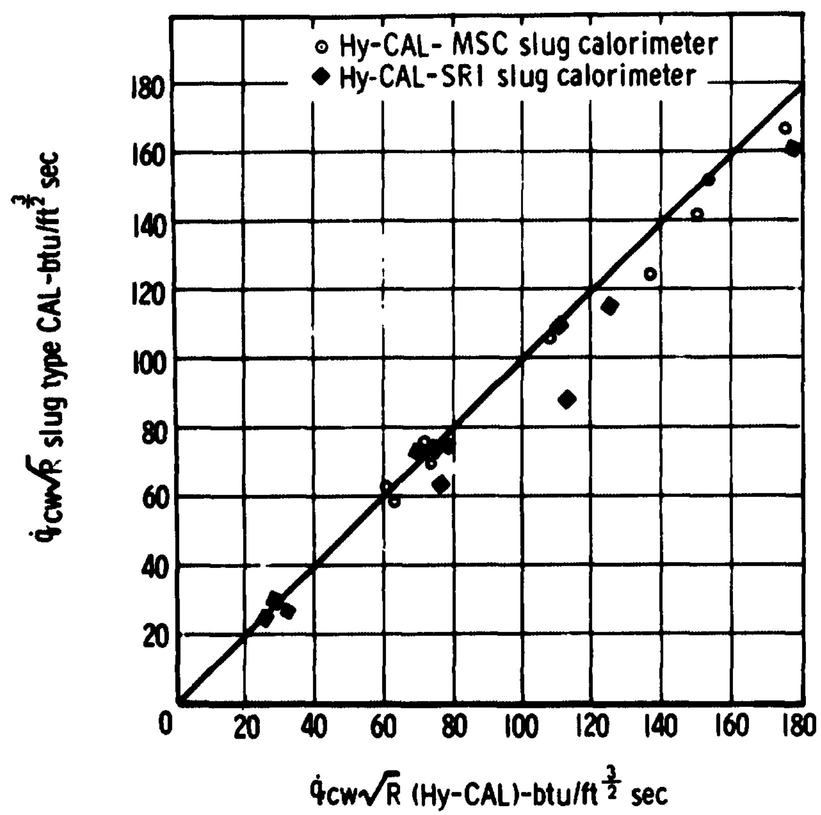

Figure 3.- Comparison of test calorimeters.

NASA-S-65-66

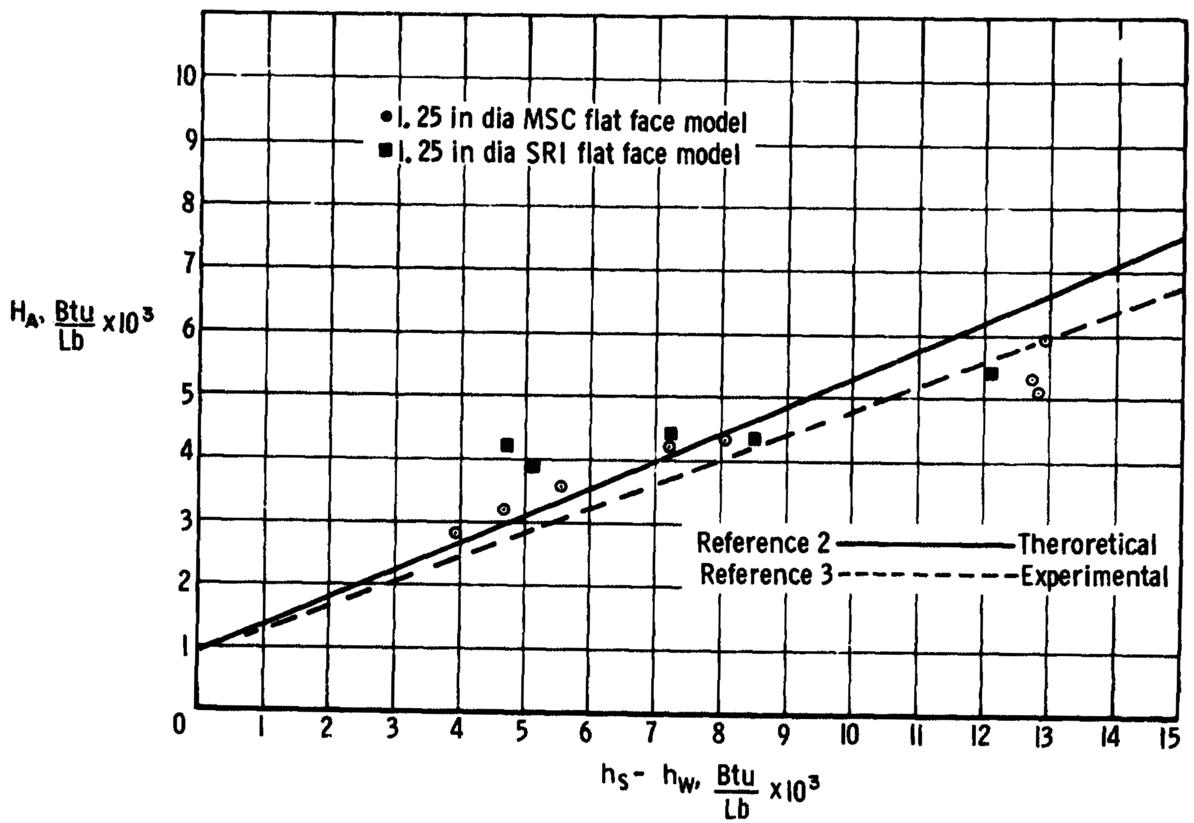

Figure 4.- Heat of ablation of teflon plotted against stagnation enthalpy potential.

NASA-S-65-67

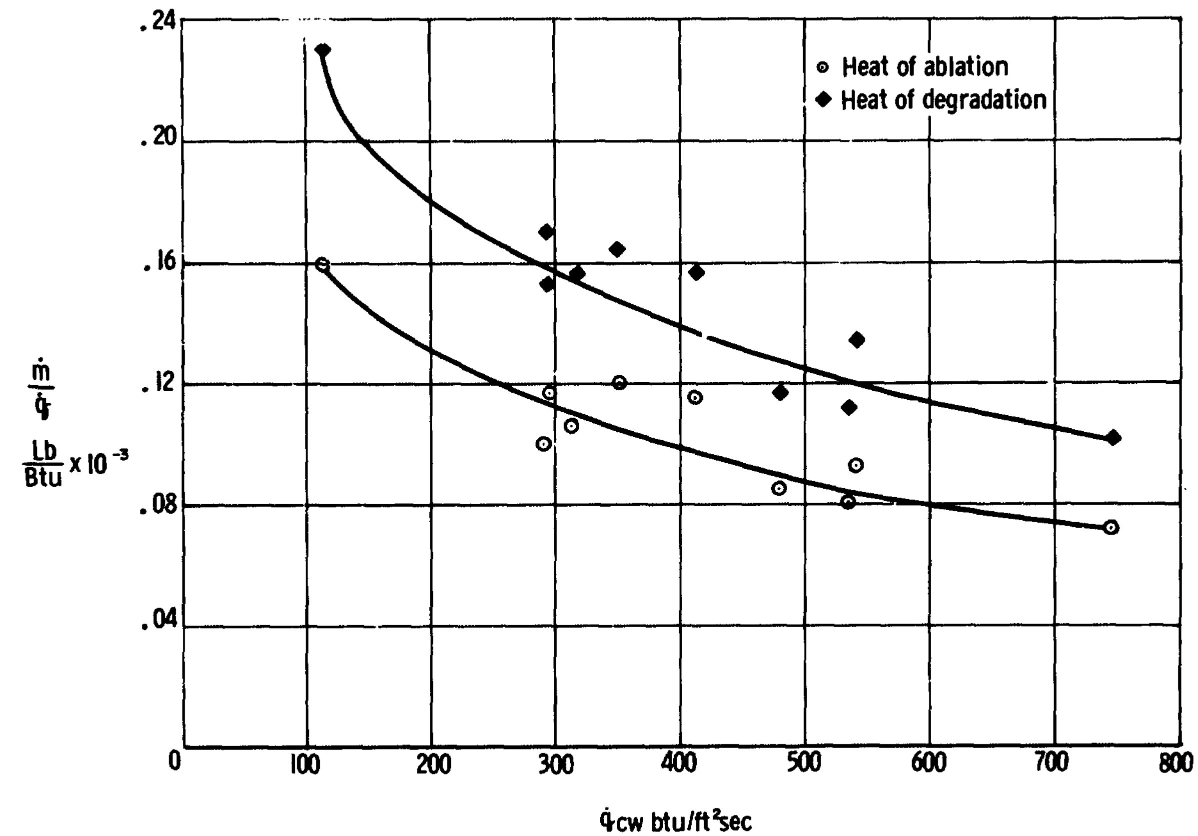

Figure 5.- Heat of degradation and ablation for phenolic nylon plotted against cold wall heating rate.

NASA-S-65-68

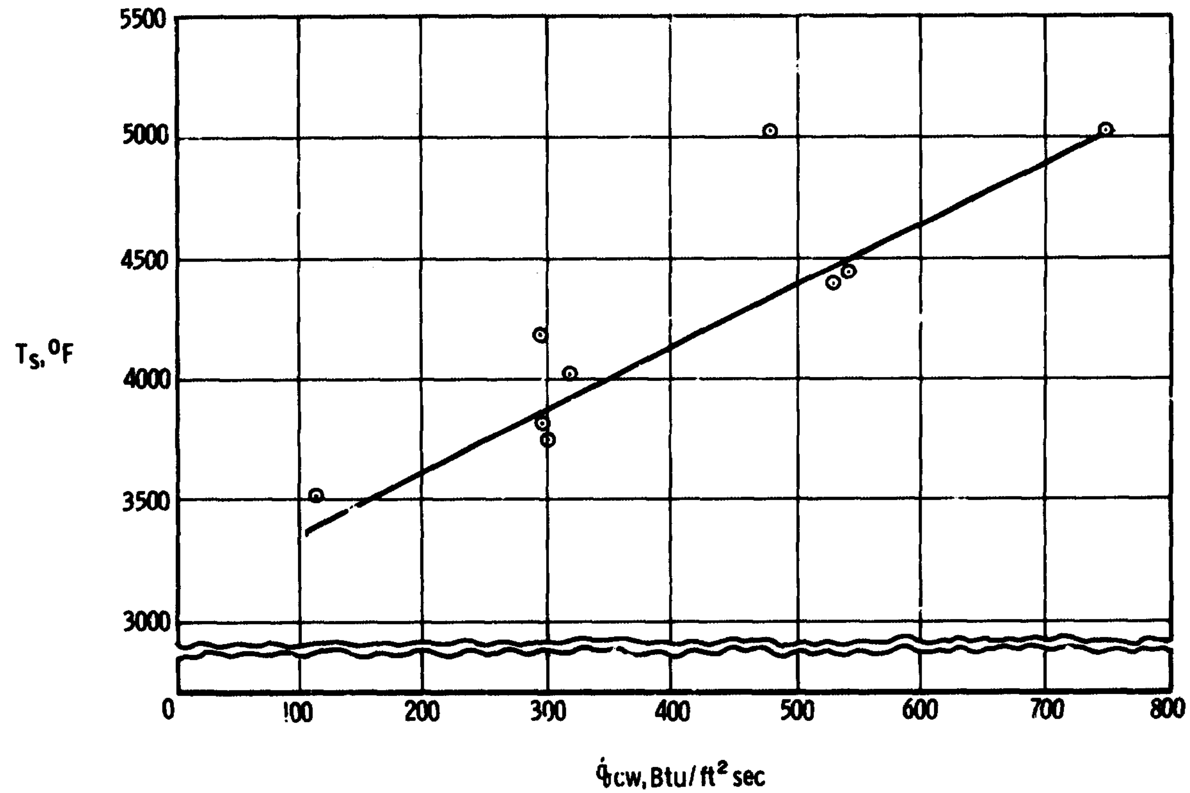

Figure 6.- Surface temperature of phenolic nylon plotted against cold wall heating rate.

NASA-S-65-72

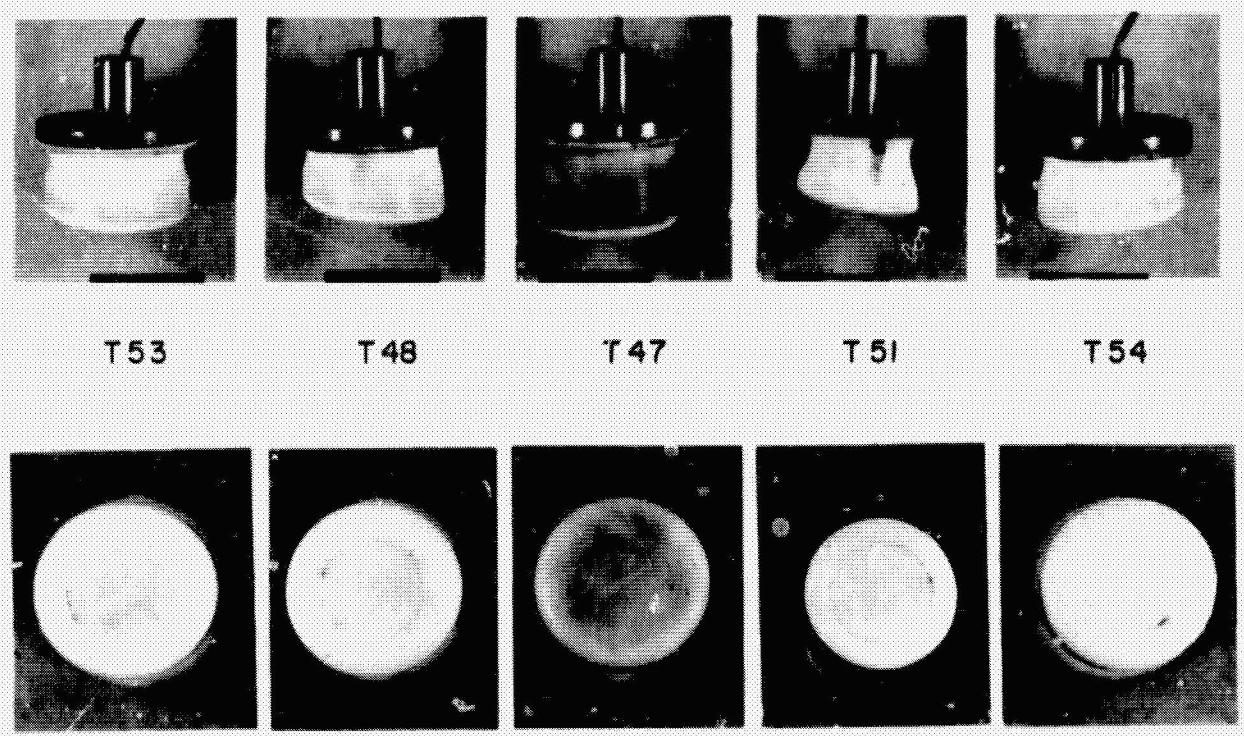

Figure 7.- Front and side views of teflon models after test.

NASA-S-65-71

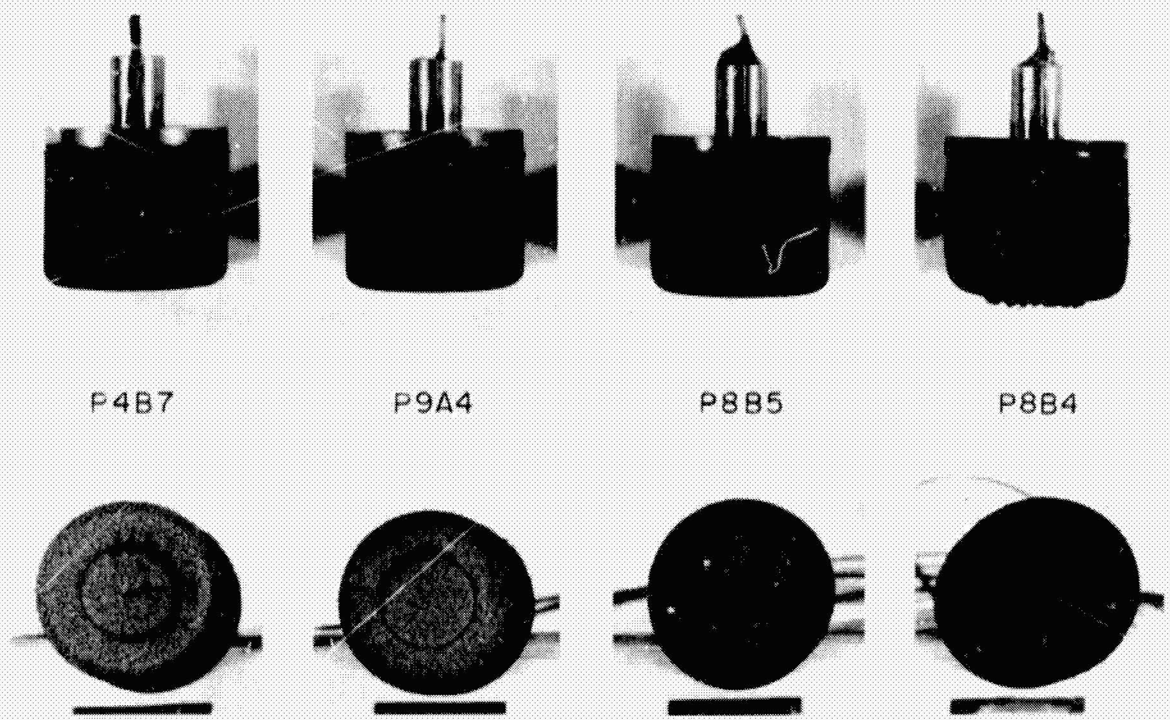

Figure 8.- Front and side views of phenolic nylon models after test.

NASA-S-65-69

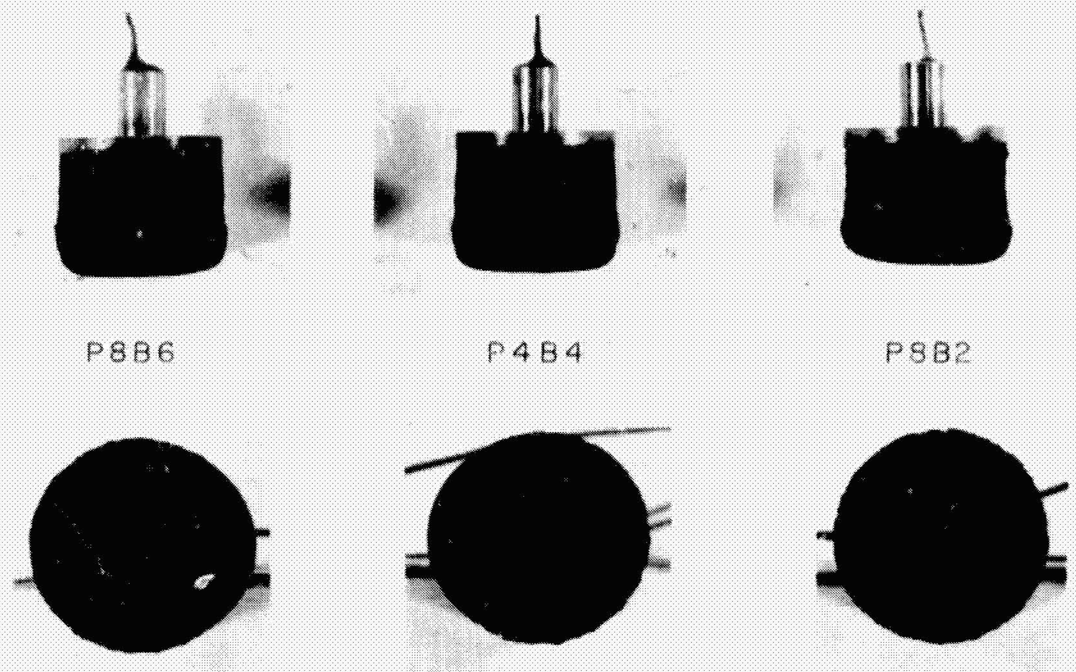

Figure 9.- Front and side views of phenolic nylon models after test.

NASA-S-65-70

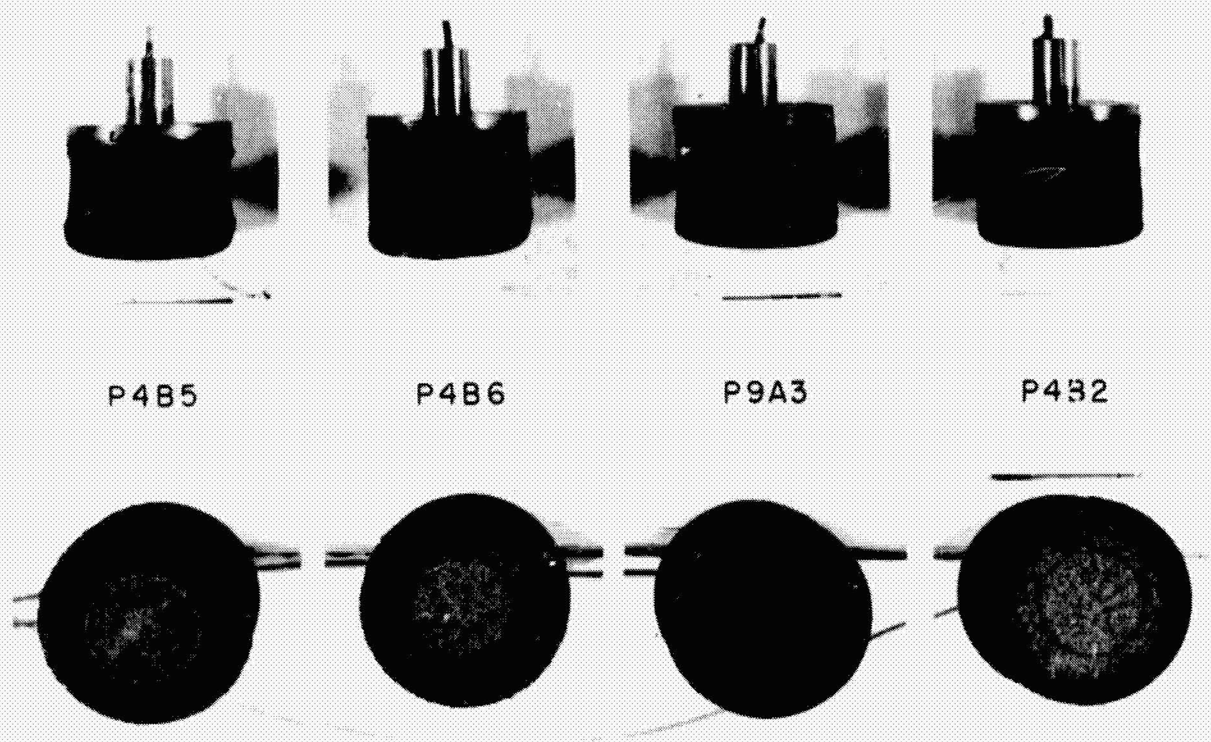

Figure 10. - Front and side views of phenolic nylon models after test.